LEGIBILITY NOTICE

A major purpose of the Technical Information Center is to provide the broadest dissemination possible of information contained in DOE's Research and Development Reports to business, industry, the academic community, and federal, state and local governments.

Although a small portion of this report is not reproducible, it is being made available to expedite the availability of information on the research discussed herein.

LA-UR-89-1760
CONF-8904216--2

Los Alamos National Laboratory is operated by the University of California for the United States Department of Energy under contract W-7405-ENG-36

LA-UR--89-1760

DE89 013461

TITLE. SPECTRA OF CRAB-LIKE PULSARS: A GRO PERSPECITVE

AUTHOR(S): Cheng Ho

SUBMITTED TO: Proceeding from GRO Workshop, Greenbelt, MD
April 10-13, 1989

DISCLAIMER

Los Alamos Los Alamos National Laboratory
Los Alamos, New Mexico 87545

SPECTRA OF CRAB-LIKE PULSARS: A GRO PERSPECTIVE

Cheng Ho
Space Astronomy and Astrophysics Group
MS D436, Los Alamos National Laboratory
Los Alamos, NM 87545

ABSTRACT

A single-parameter model has been constructed to calculate the continuum spectrum of energetic pulsed radiation resulted from the formation of a Crab-type charge depletion region (gap) in the outer magnetosphere of rapidly spinning pulsars (Ho 1989). We discuss the characteristics of the theoretical predictions for the Crab pulsar and the specific features expected in the energy bands of the Gamma-Ray Observatory (GRO). These features include (1) a possible spectral dip in the 0.3 to 30 MeV range, (2) a change in polarization behavior below and above the dip, if polarization can be discerned, and most importantly, (3) an exponential roll-over in the energy range greater than several GeV. The EGRET detector of GRO covers the energy range necessary to detect the exponential roll-over. This model predicts that the 50-ms pulsar in the Large Magellanic Cloud (PSR0540−693) will be marginally detectable by GRO with a nominal two-week integration. Furthermore, we discuss the spectrum and detectability of a pulsar with 0.5 ms period and a surface magnetic field of 10^9 G. Such pulsar may exist in SN 1987A. Since the 50-ms pulsar and SN 1987A are within the same field of view of GRO, it will be of great importance to take an extra long integration of this region to search for gamma-ray emission from these sources.

I. INTRODUCTION

Rapidly spinning neutron stars with substantial magnetic dipole moments are known to be powerful emitters of radiation in energy bands much higher than radio frequencies. Two of the three definitely identified discrete γ-ray sources in the energy range greater than 3 MeV fall into this category: the Crab pulsar and the Vela pulsar. The third discrete γ-ray point source, "Geminga," could be an aligned fast pulsar, which, because of the alignment, has eluded detection of its expected short period (Ruderman and Cheng 1988).

To explain the origin and mechanism of the energetic radiation from these pulsars, a model has been proposed based on the formation of a finite region of vacuum (gap) in the outer magnetosphere (Cheng, Ho and Ruderman 1986*a* and 1986*b*; hereafter Paper I and Paper II). In Papers I and II, detailed considerations of the electrodynamics, radiation mechanisms, and charge production processes of the gap indicate that the Crab pulsar and the Vela pulsar work under a very different set of parameters and mechanisms. The Crab-type gap produces GeV photons via curvature radiation and subsequently produce $e^{\pm}$ which radiate synchrotron radiation and inverse-Compton-scattered photons. The 50-ms pulsar PSR0540−693 (Seward, Harnden, and Helfand 1982) in the Large Magellanic Cloud is probably powered by a Crab-type gap. The Vela-type gap produces primary photons with energies greater than several TeV via inverse Compton scattering and subsequently produce $e^{\pm}$ which radiate synchrotron radiation up to the GeV range. The 150-ms pulsar PSR1509−58 (Seward and Harnden 1982) is probably powered by a Vela-type gap. In this paper, we shall concentrate on pulsars with a Crab-type outer gap.

In Paper II, the continuum spectrum of pulsed radiation was calculated for the Crab pulsar and the result agreed semi-quantitatively with observations. However, that calculation was specific to the Crab pulsar and had little predictive power. To remedy these shortcomings, a single-parameter model has been constructed to calculate the spectra from the Crab-type outer gap without using observational data as input (Ho 1989, hereafter Paper III). In § II, we review the radiation processes, charge production mechanisms and spectral calculation for the Crab-type outer gap described in Papers I, II and III. Section III discusses the spectrum of the

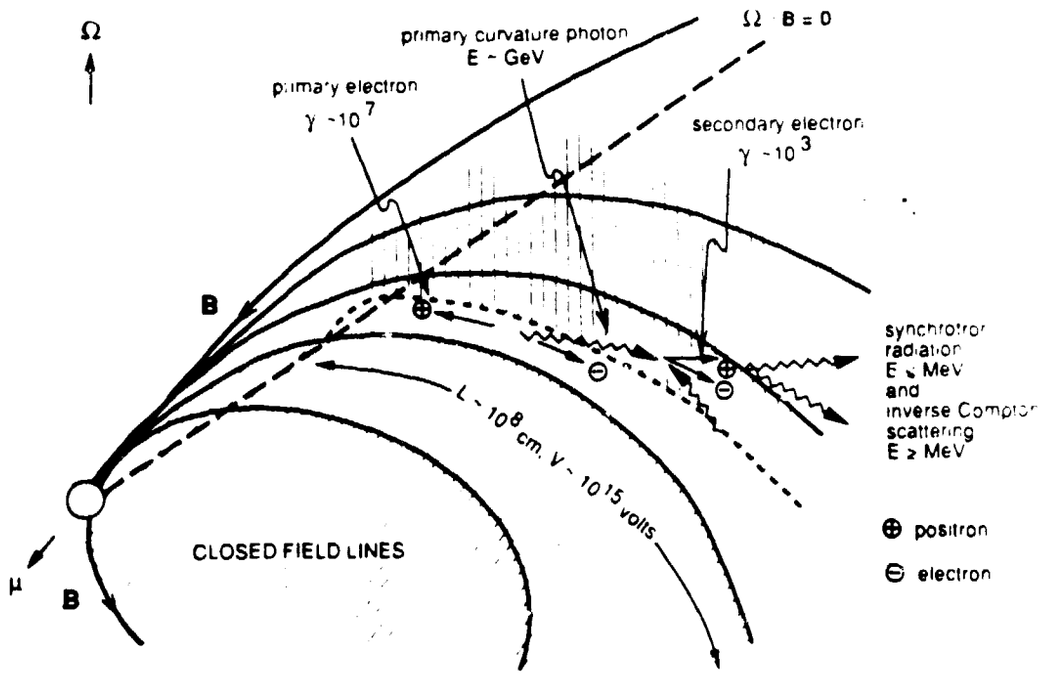

Figure 1 – Schematics of the Crab-type outer gap. The outer gap resides above the closed-field-line region (diagonally shaded region) and the short-dash line. For the Crab pulsar, the gap has a length of $\sim 10^8$ cm and a voltage drop of $\sim 10^{15}$ volts. Electrons inside the gap are accelerated to relativistic energy and radiate curvature radiation with characteristic energy about several GeV. Secondary electrons are created in the secondary region (vertically shaded region), via γ-γ annihilation between GeV and keV photons. Synchrotron radiation and inverse Compton scattering combine to yield the emergent spectrum.

Crab pulsar. Section IV gives the results for the 50-ms pulsar. Section V discusses the range of parameters for a 0.5-ms pulsar in SN 1987A and gives the results for a hypothetical pulsar with 0.5 ms periodicity and a 10^9 G surface magnetic field. Special emphases are put on the observations to be made by GRO. A discussion and summary are given in § VI.

II. OVERVIEW OF THE MODEL

In this section, we review the essence of the Crab-type outer gap proposed in Paper I and II, and the calculation of the spectrum of pulsed radiation discussed in Paper III. For more detailed discussions, see Papers I, II and III.

An outer gap is an extensive region of vacuum near the light cylinder ($r = c/\Omega$) which results from current flows along the open field lines. Figure 1 schematically shows the location and structure of the Crab-type outer gap. A gap of height a will induce an electric field with substantial component parallel to the magnetic field. The maximum parallel electric field is

$$E_{max} = \Omega B a^2 / 4sc, \tag{1}$$

and the maximum potential drop along the gap is

$$V_{max} = \Omega B a^2 L / 4sc, \tag{2}$$

where s is the radius of curvature of the field lines, Ω is the angular frequency of the pulsar, B is the local magnetic field strength, and L is the length of the gap. The gap is bounded from below by the last closed field line assumed to be dormant with a static surface charge density

$$\Sigma = \Omega B a x / 4\pi c, \tag{3}$$

where x is the distance along the gap. The upper boundary of the gap resides in the region threaded by open field lines and is not static. Electric current flows along it and constant charge production and separation maintain the surface charge density prescribed by Eq. (3). The current in the upper boundary is given by

$$I \simeq \Omega B a W L / 4\pi s, \tag{4}$$

where W is the breadth of the gap. The surface charge density on the upper and lower boundaries shields the gap from the rest of the magnetosphere (see Paper I for more details).

In a Crab-type gap, "primary electrons" accelerated by the electric field of the gap (Eq. [2]) contribute to the electric current (Eq. [3]) and radiate predominantly through curvature radiation ("primary photons") as they move along the curved magnetic field line. These primary photons typically have energy around several GeV and they annihilate, via photon-photon annihilation, into $e^{\pm}$ pairs ("secondary electrons"), over a large spatial area when they encounter a flux of keV X-ray photons in the head-on direction. The secondary electrons, with substantial perpendicular momentum, emit synchrotron radiation typically into energy bands below several MeV. The secondary electrons inverse-Compton scatter the X-ray synchrotron radiation emitted by the crossing beam of secondary electrons into the energy band greater than several MeV. These two components, synchrotron and inverse-Compton, combine to yield the emergent spectrum ("secondary photons").

The spectrum of pulsed radiation from the Crab pulsar was calculated in Paper II, in which two steps were taken. (1) Observed spectra was used as an input. (2) Three parameters were employed: the energy of the primary electrons, the local magnetic field strength, and the overall normalization. The calculated spectrum agrees with that observed semi-quantitatively. However, that calculation cannot be extended to other pulsars due to the lack of broad-band observational data, and allowing three varying parameters reduces the constraining capability of the model. To remedy these shortcomings, a computational model has been constructed in Paper III which (1) eliminates the need to use observational data and (2) reduces the number of free parameters to one.

In Paper III, the gap is parameterized by the linear fraction of the gap:

$$f_G \equiv a/s. \tag{5}$$

The available potential drop along a gap with size f_G is given by equation (2) and the current in the upper boundary is given by equation (4). We assume that the maximum potential drop along the gap is completely accessible by the current in the upper boundary of the gap. The total potential drop along the gap determines the energy of the primary electron; the total current determines the overall normalization. For definiteness, we take

$$s = W = L = R_{LC} = c/\Omega \tag{6}$$

and

$$B = \mu R_{LC}^{-3}, \tag{7}$$

where μ is the dipole moment of the pulsar. We employ iteration to eliminate the need to use observational data as input. The spectrum typically converges after six iterations and the computation has been tested to check that the result is independent of the initial condition.

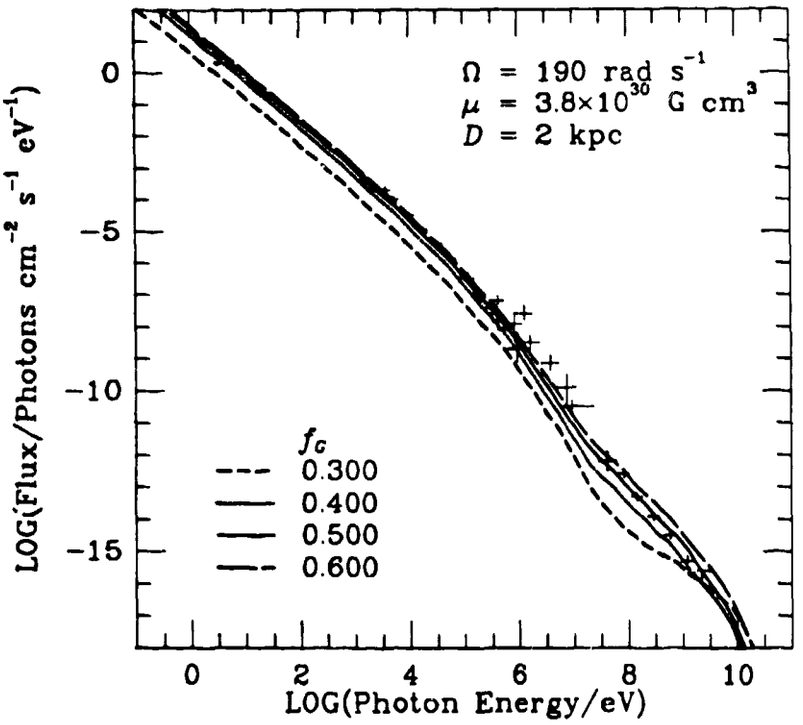

Figure 2 — Theoretical spectra of the Crab pulsar after 10 iterations with f_G = 0.3, 0.4, 0.5, and 0.6. Note the similarity in general features of these spectra with those shown in Fig. 6 of Paper II. See also Footnote 1. (Observation data are from Oke 1969; Kestenbaum *et al.* 1970; Fritz *et al.* 1971; Knight 1982; Mahoney, Ling and Jacobson 1983; Clear *et al.* 1987.)

Summarizing this overview, for a fast pulsar with given Ω and μ, which are directly observable and inferred from the spin-down rate, the broad-band spectrum of pulsed radiation can be calculated with only one dimensionless parameter: f_G. Folding in the distance D to the pulsar, the model predicts the flux of pulsed radiation which can be compared with observations. Results for the Crab pulsar, the 50-ms pulsar and a hypothetical 0.5-ms pulsar in SN 1987A will be given in the following sections.

III. THE CRAB PULSAR

The Crab pulsar has the following parameters: $\Omega = 190$ rad s^{-1}, $\mu = 3.8 \times 10^{30}$ G cm^3, and $D = 2$ kpc. The theoretical spectra of the Crab pulsar after 10 iterations for $f_G = 0.3$, 0.4, 0.5 and 0.6 are shown in Fig. 2, along with the observed fluxes.[1] The general features of the spectra coincide with those presented in Fig. 6 of Paper II. They include (1) a synchrotron-radiation component which can be described by a power law with a slowly-varying power-law index at the low energy end and (2) a component from the inverse Compton scattering at the high energy end. The two components overlap at a photon energy between 300 keV and 30 MeV which produce a broad dipping feature in the spectrum. The prominence and location of the dip and the ratio of the two components are a function of the gap fraction.

Judging from Fig. 2, the spectrum calculated from $f_G = 0.5$ appears to give the best fit ("by eye") to the observations. Overall, spectra from $0.4 < f_G < 0.6$ yield acceptable fits in the sense that at no place does the predicted spectrum consistently deviate from the observations by

[1] In Paper III, the spectra presented for the Crab pulsar were calculated with the secondary photons fully participating in the process of generating the secondary electrons, while the spectra for the 50-ms LMC pulsar were calculated with no participation of secondary photons in the charge production process. This is the cause of the slight enhancement of the low energy part of the spectrum in Figure 3 of Paper III, compared to those in Figure 2 of this paper. Within this paper, we uniformly suppress the participation of secondary photons in the charge production process, since Figure 2 appears to yield better fit to the observations. The closure *Ansatz* discussed in §V of Paper III remains valid.

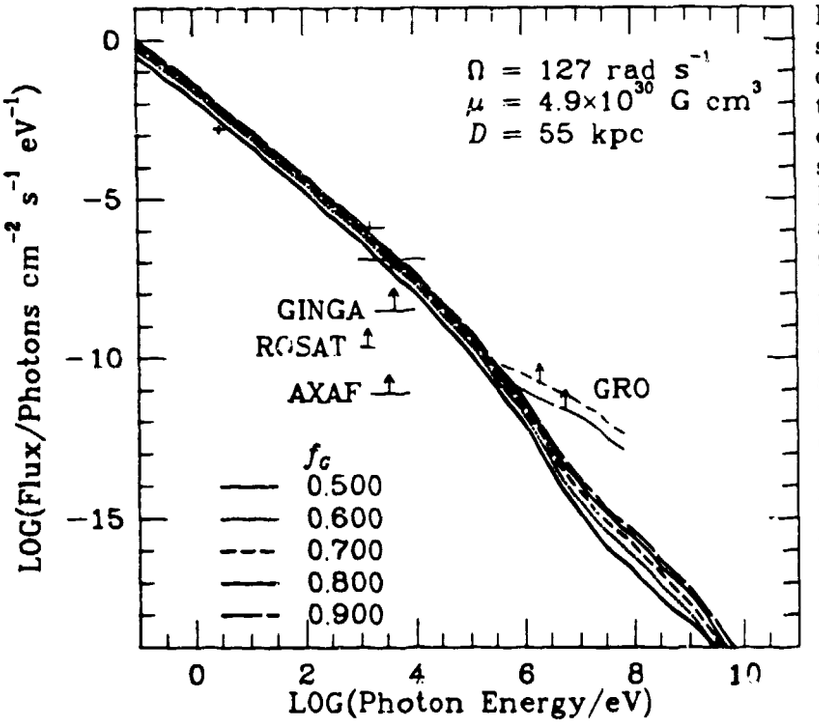

Figure 3 — Theoretical spectra of the 50 millisecond pulsar in the LMC after 10 iterations with various values of f_G. DC sensitivities of the satellites ROSAT (PSPC), AXAF and *Ginga* (LAC) for a 10^5 sec integration are plotted. Also shown is the sensitivity of GRO (OSSE) for detecting a Crab-like pulsar (*solid line*) and a pulsar with a duty cycle of 0.5 (*dashed line*, Knight *et al.* 1982), for a 10^6 sec integration. (Observational data are from Middleditch and Pennypacker 1985, Seward, Harnden and Helfand 1984, and Inoue *et al.* 1988.)

much more than an order of magnitude for over more than a decade of emergent photon energy. In view of the small number of parameters and the wide coverage in photon energy, we consider the agreement between the theory and observation satisfactory. Accepting the spectra with f_G between 0.4 and 0.6 as reasonable fits to the observations, comparison between the predicted and observed spectra serve as a fiducial estimate to the theoretical uncertainty. For the Crab pulsar, the model leads to a spectrum which (1) overestimates the optical flux by a factor of about 10, (2) underestimates the flux between 1 keV and 300 keV by a factor less than 3, (3) underestimates the flux between 300 keV and 10 MeV by a factor of about 10, and 4) is within a factor of 2 of the observed flux above 10 MeV.

IV. THE 50-MS PULSAR IN LMC (PSR0540−693)

The parameters for PSR 0540−693 are: $\Omega = 127$ rad s^{-1}, $\mu = 4.9 \times 10^{30}$ G cm^3, and $D = 55$ kpc. Theoretical spectra for $f_G = 0.5$, 0.6, 0.7, 0.8, and 0.9 after 10 iterations are shown in Fig. 3. The parameters f_G between 0.7 and 0.9 yield spectra which fit the existing optical and X-ray observation in the same fashion as for the Crab pulsar, i.e., overestimates the optical flux and slightly underestimates the X-ray flux. For comparison, we have plotted the sensitivities for detecting a DC source by ROSAT (PSPC) and AXAF for a 10^5 sec integration (Trümper 1984), the sensitivity for a DC source by *Ginga* (LAC) with a 10^5 sec integration (Makino *et al.* 1987), and the sensitivity of detecting a Crab-like pulsar by GRO (OSSE) for a 10^6 sec integration (Kurfess *et al.* 1983). Despite the crowdedness of the large field of view of LAC near the LMC pulsar (which contains SN 1987A, among other X-ray point sources), pulsation has been detected by *Ginga* (Dotani *et al.* 1988, Inoue *et al.* 1988). Judging from Fig. 3, the LMC pulsar is undetectable by OSSE, with a duty cycle of ~ 0.5. However, the theory underestimates the pulsed flux at ~ 1 MeV by a factor of ~ 10 for the Crab pulsar. Allowing for the same increase by a factor of 10, the γ-ray pulsation could be readily detected by OSSE, especially at energies below 1 MeV.

V. A 0.5-MS PULSAR IN SN 1987A

The detection of neutrinos from the supernova 1987A suggests the formation of a neutron star. Recently, Middleditch *et al.* (1989) reported the detection of a very strong modulation

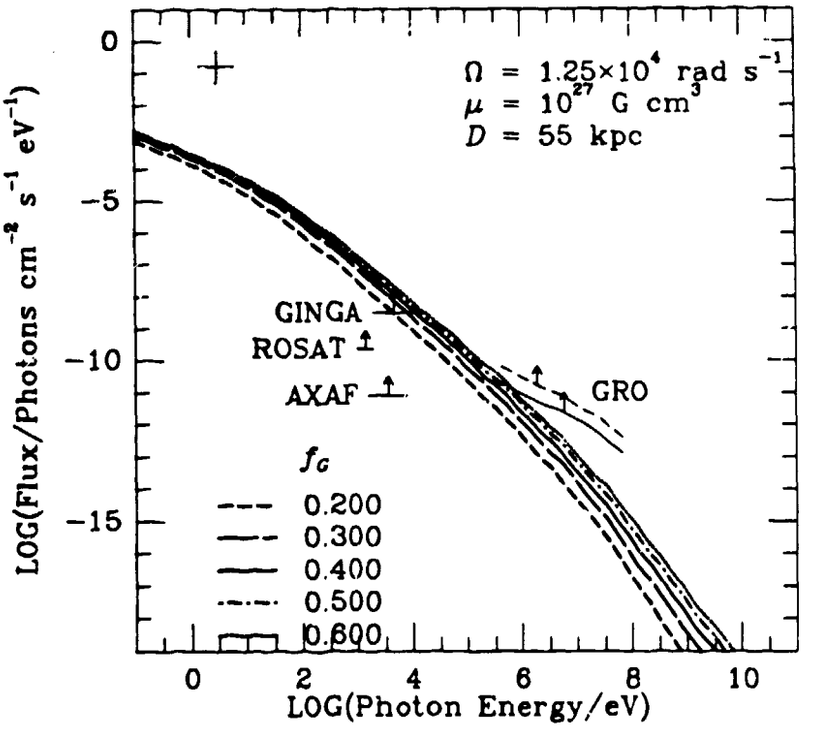

Figure 4 — Theoretical spectra of PSR Z after 10 iterations with f_G = 0.2, 0.3, 0.4, 0.5, and 0.6. The estimated pulsed flux (Middleditch 1989) is presented for the purpose of comparison. It should be treated as tentative pending confirmation.

at a frequency of about 2 kHz from SN 1987A during a seven-hour observing run. Subsequent attempts for confirmation have failed thus far. We now consider the observable consequences of a 0.5-ms pulsar in the Large Magellanic Cloud. The outer gap model requires an input of the magnetic dipole moment of the neutron star which has not been determined. In the following, we estimate the allowable range of μ based on current observations. *If* the 0.5-ms pulsar acts like the Crab pulsar, which dumps most of its rotational energy loss into the nebula, *and* the observed light from SN 1987A is a good indicator of the amount of energy input from the center of the supernova, *then*

$$\frac{\Omega^4 \mu^2}{c^3} \simeq I \Omega \dot{\Omega} \lesssim \dot{E}_{\rm SN1987A} \lesssim 10^{39} \text{ ergs s}^{-1}, \tag{8}$$

where I is the moment of inertia of the neutron star and taken to be 10^{45} g cm^2. We have used the estimate given by Pinto, Woosley, and Ensman (1988). More recent observations put an even more stringent limit on μ (Hartmann, Woosley, and Pinto 1989). *On the other hand*, the pulsar cannot be losing more energy in pulsation than in total rotational energy loss, *thus*

$$\frac{\Omega^4 \mu^2}{c^3} \simeq I \Omega \dot{\Omega} > \dot{E}_{\rm optical\ pulsation} \gtrsim 10^{35} \text{ ergs s}^{-1}. \tag{9}$$

Here we have adopted a highly conservative estimate of the power in optical pulsation during the detection; the actual luminosity of the pulsed emission during the 7-hour detection can be greater than this estimate by as much as a factor of ten (Middleditch 1989). Combining equations (8) and (9), the 0.5-ms pulsar has a magnetic dipole in the following range:

$$10^{25} \text{ G cm}^3 < \mu < 10^{27} \text{ G cm}^3. \tag{10}$$

We now consider a *hypothetical* pulsar in the LMC with a period of 0.5 ms and a dipole moment at the upper end of the estimated range: $\Omega = 1.25 \times 10^4$ rad s^{-1}, $\mu = 10^{27}$ G cm^3, and D = 55 kpc. We shall refer to this hypothetical pulsar as PSR Z.

Theoretical spectra for PSR Z with f_G=0.2, 0.3, 0.4, 0.5, and 0.6 are plotted in Figure 4. The optical flux is a very rough estimate with great uncertainty. It is presented only for the purpose of comparison. From Fig. 4, the theoretical prediction for optical pulsation is off by orders of magnitude. This discrepancy appears to be difficult to reconcile without introducing a new radiation mechanism in the optical range. One possibility is the coherent curvature radiation by clumps of GeV secondary electrons, in analogy to the mechanism of radio emission proposed for the older radio pulsar (Ruderman and Sutherland 1975). The spectra presented in Figure 4 predict a γ-ray flux which is marginally detectable. The pulse profile of SN 1987A pulsar is expected to be similar to tha. of the Crab pulsar, based on the similarity of the structure of the Fourier components (Middleditch 1989). A sharp pulse profile like that of the Crab pulsar would make PSR Z more readily detectable than the 50-ms pulsar.

VI. DISCUSSION AND SUMMARY

We now discuss the theoretical predictions observable by GRO and implications of GRO observations to the theory.

For the Crab pulsar, the basic spectral shape is well established. GRO can be utilized for the detailed study of the spectral structure and test the validity of the outer gap model. The outer gap model predicts two features with significant theoretical implications in the energy band of GRO. The first feature is the dip at the overlap of the synchrotron component and the inverse-Compton component. As shown in Fig. 2, the dip is broad with varying prominence depending on the gap size. GRO observations in the γ-ray range will allow us to put constraints on the parameter f_G. Furthermore, polarization of the radiation could serve as an even stronger telltale sign of a two-component spectrum. The synchrotron-radiation component at lower-energy is expected to be polarized. This is seen in the phase-resolved observations of the optical pulses from the Crab pulsar (Manchester and Taylor 1977). The maximum polarization is observed in the wings of the optical pulses at about 20 to 30 per cent. This serves as an indication of the expected degree of polarization for the synchrotron γ-ray emission. It is crucial that the observation be made with sufficient phase resolution. On the other hand, the inverse-Compton component consists of reprocessed synchrotron radiation. The polarization is difficult to evaluate without a detailed model of the emission geometry in the azimuthal dimension. Intuitively, one would expect the reprocessed radiation to be less polarized. An observation of the polarization will provide important input and allow us to study the three-dimensional structure of the gap in detail. Feasibility of obtaining polarization information of γ rays has been reported with detection of finite polarization from the Vela pulsar (Caraveo *et al.* 1988). We note that the spectral dip and the different polarization behavior below and above the dip are expected features from any two-component model for the broad-band spectrum. GRO provides a unique opportunity for this study with its wide energy coverage of more than four orders of magnitude.

The second feature in the Crab pulsar spectrum is roll-over in the multi-GeV range. The roll-over occurs for two reasons. (1) The secondary electrons are created from the primary photons which follows a curvature radiation spectrum. Thus the secondary-electron distribution is cut off by an exponential roll-over above several GeV, the characteristic energy of the primary curvature radiation. Since inverse-Compton scattering cannot produce photons with energies greater than the seed electron, we expect the emergent spectrum to exhibit a similar exponential roll-over. (2) The outer gap model predicts two beams of electrons and photons crossing each other in the secondary region. Any multi-GeV secondary photon will experience pair-production attenuation as it encounters an opposing beam of sub-keV photons, in analogy to the conversion of primary photons to secondary electrons. This will be manifested as a sharp and most likely exponential turn-off at the high-energy end of the emergent spectrum. Theoretical spectra presented in Fig. 2 do not include the effect of such attenuation, since a more detailed model of geometry of the secondary region is required. Both effects predict a spectral roll-over in the multi-GeV regime. The first effect is unique to the Crab-type gap. The second effect is

general for any cross-beaming geometry. A detailed study of the pulsed spectrum in the multi-GeV regime by EGRET will allow us to test the validity of the Crab-type outer gap picture, place constraints on the parameter f_G, consider the importance of the cross-beaming effect, and construct a more realistic picture of the geometry.

For the 50-ms and 0.5-ms pulsars, the outer gap model predicts that they are marginally detectable. Since PSR0540−693 and SN 1987A are within the same fields of view of all instruments on GRO, long integration in their neighborhood will have an added advantage of killing two birds with one stone. *In fact, because of their compact angular size and close proximity to us, long integrations of the Magellanic Clouds may be the best investment for discovering discrete γ-ray sources by GRO.* Once the presence of γ-ray pulsation from either sources is established, a number of subsequent multi-wavelength studies should be vigorously pursued with coordinated effort between GRO, HST, ROSAT, and ground-based radio, optical and ultra-high-energy telescopes. The multi-wavelength studies, including the compilation of the spectrum, the comparison of the pulse profile and pulse arrival time at different energy bands, and the long-term monitoring of the pulsar, will provide invaluable input toward our understanding of the pulsar phenomenon.

I thank John Middleditch for helpful conversations and Chris Mauche for comments on the manuscript. This work was performed under the auspices of U.S. Department of Energy.

REFERENCES

Caraveo, P. A., *et al.*, 1988, *Ap. J.*, **327**, 203.

Cheng, K. S., Ho, C., and Ruderman, M., 1986, *Ap. J.*, **300**, 500 (Paper I).

Cheng, K. S., Ho, C., and Ruderman, M., 1986, *Ap. J.*, **300**, 522 (Paper II).

Clear, J., *et al.*, 1987, *Astr. Ap.*, **174**, 85.

Dotani, T. *et al.*, 1988, *Proc. Int'l Symp. on the Phys. of Neutron Stars and Blackholes*, ed. Y. Tanaka, (Tokyo: Univ. Acad. Press).

Fritz, G., *et al.*, 1971, *Ap. J.(Letters)*, **164**, L55.

Hartmann, D., Woosley, S. E., and Pinto, P. A., 1989, these proceedings.

Ho, C., 1989, *Ap. J.*, **342**, in press (Paper III).

Inoue, H., *et al.*, 1988, private communication.

Kestenbaum, H. L., Ku, W., Novick, R., and Wolff, R. S. 1976, *Ap. J.(Letters)*, **203**, L57.

Knight, F. K., 1982, *Ap. J.*, **260**, 538.

Knight, F. K., Matteson, J. L., Peterson, L. E., and Rothschild, R. E., 1982, *Ap. J.*, **260**, 553.

Kurfess, J. D. *et al.*, 1983, *Adv. Sp. Res.*, **3**, 109.

Mahoney, W. A., Ling, J. C., and Jacobson, A. S., 1984, *Ap. J.*, **278**, 784.

Makino, F. and the Astro-C team, 1987, Institute of Space and Astronautical Science, Japan, Research Note 326.

Manchester, R. N., and Taylor, J. H., 1977, *Pulsars* (San Francisco: Freeman).

Middleditch, J., and Pennypacker, C., 1985, *Nature*, **313**, 659.

Middleditch, J., *et al.*, 1989, *IAU Cir.* 4735.

Middleditch, J., 1989, private communication.

Oke, J. B., 1969, *Ap. J.(Letters)*, **156**, L49.

Pinto, P. A., Woosley, S. E., and Ensman, L. M., 1988, *Ap. J.(Letters)*, **331**, L101.

Ruderman, M. and Sutherland, P., 1975, *Ap. J.*, **196**, 51.

Ruderman, M., and Cheng, K. S., 1988, *Ap.J*, **335**, 306.

Seward, F. D., and Harnden, F. R., Jr., 1982, *Ap. J.(Letters)*, **262**, L31.

Seward, F. D., Harnden, F. R., Jr., and Helfand, D.J. 1984, *Ap. J.(Letters)*, **287**, L19.

Trümper, J., 1984, *Phys.Scr.*, **T7**, 209.